

Synthesis, Characterization, and Spectroelectrochemistry of Cobalt Porphyrins Containing Axially Bound Nitric Oxide

George B. Richter-Addo,^{*,†} Shelly J. Hodge,[†] Geun-Bae Yi,[†] Masood A. Khan,[†] Tianshu Ma,[‡] Eric Van Caemelbecke,[‡] Ning Guo,[‡] and Karl M. Kadish^{*,‡}

Department of Chemistry and Biochemistry, University of Oklahoma, 620 Parrington Oval, Norman, Oklahoma 73019, and Department of Chemistry, University of Houston, Houston, Texas 77204-5641

Received January 11, 1996[®]

Several cobalt nitrosyl porphyrins of the form (T(*p/m*-X)PP)Co(NO) (*p/m*-X = *p*-OCH₃ (**1**), *p*-CH₃ (**2**), *m*-CH₃ (**3**), *p*-H (**4**), *m*-OCH₃ (**5**), *p*-OCF₃ (**6**), *p*-CF₃ (**7**), *p*-CN (**8**)) have been synthesized in 30–85% yields by reaction of the precursor cobalt porphyrin with nitric oxide. Compounds **1–7** were also prepared by reaction of the precursor cobalt porphyrin with nitrosonium tetrafluoroborate followed by reduction with cobaltocene. Compounds **1–8** have been characterized by elemental analysis, IR and ¹H NMR spectroscopy, mass spectrometry, and UV–vis spectrophotometry. They are diamagnetic and display ν_{NO} bands in CH₂Cl₂ between 1681 and 1695 cm⁻¹. The molecular structure of **1**, determined by a single-crystal X-ray crystallographic analysis, reveals a Co–N–O angle of 119.6(4)°. Crystals of **1** are monoclinic, *P*2₁/*c*, with *a* = 15.052(1) Å, *b* = 9.390(1) Å, *c* = 16.274(2) Å, β = 111.04(1)°, *V* = 2146.8(4) Å³, *Z* = 2, *T* = 228(2) K, *D*(calcd) = 1.271 g cm⁻³, and final *R*1 = 0.0599 (*wR*2 = 0.1567, GOF = 1.054) for 3330 “observed” reflections with *I* ≥ 2σ(*I*). Cyclic voltammetry studies in CH₂Cl₂ reveal that compounds **1–7** undergo two reversible oxidations and two reversible reductions at low temperature. This is not the case for compound **8**, which undergoes two reversible reductions but an irreversible oxidation due to adsorption of the oxidized product onto the electrode surface. Combined electrochemistry–infrared studies demonstrate that each of the compounds **1–7** undergoes a first oxidation at the porphyrin π ring system and a first reduction at either the metal center or the nitrosyl axial ligand. The formulation for the singly oxidized products of compounds **1–7** as porphyrin π-cation radicals was confirmed by the presence of bands in the 1289–1294 cm⁻¹ region (for compounds **1–5**), which are diagnostic IR bands for generation of tetraarylporphyrin π-cation radicals.

Introduction

Studies into the binding of nitric oxide (NO) by metalloporphyrins have aided our understanding of how NO interacts with heme-containing biomolecules, such as hemoglobin, myoglobin, and soluble guanylate cyclase.^{1–4} Many iron nitrosyl porphyrins have been examined as model compounds during such studies,^{5,6} but other metalloporphyrins are also known to form nitrosyl derivatives.⁷ Although they have not been studied as much as their iron analogs, cobalt nitrosyl porphyrins have also gained

prominent attention for the binding and activation of nitric oxide. For example, the water-soluble [(2-TMPyP)Co(NO)]⁴⁺ (2-TMPyP = (*N*-methyl-2-pyridiniumyl)porphyrin) has been prepared and its [(2-TMPyP)Co]⁵⁺ precursor shown to be a good electrocatalyst for NO and nitrite reduction.⁸ Furthermore, (TPP)Co (TPP = the dianion of tetraphenylporphyrin) supported by TiO₂ or imidazole/SiO₂ is unusually active for the reduction of NO by carbon monoxide or hydrogen, respectively.⁹

The substitution of iron by cobalt in heme and synthetic porphyrins has also gained attention in a biological setting. For example, (TPP)Co(NO) has been explored as an isoelectronic model for oxygenated protoheme.¹⁰ The NO adducts of cobalt-substituted myoglobin and hemoglobin are also known.¹¹ Fajer

[†] University of Oklahoma.

[‡] University of Houston.

[®] Abstract published in *Advance ACS Abstracts*, October 1, 1996.

- (1) (a) Stone, J. R.; Marletta, M. A. *Biochemistry* **1994**, *33*, 5636 and references therein. (b) Wang, J.; Rousseau, D. L.; Abu-Soud, H. M.; Stuehr, D. J. *Proc. Natl. Acad. Sci. U.S.A.* **1994**, *91*, 10512. (c) Ignarro, L. J. *Semin. Hematol.* **1989**, *26*, 63. (d) Craven, P. A.; DeRubertis, F. R. *Biochim. Biophys. Acta* **1983**, *745*, 310. (e) Craven, P. A.; DeRubertis, F. R. *J. Biol. Chem.* **1978**, *253*, 8433. (f) Hurshman, A. R.; Marletta, M. A. *Biochemistry* **1995**, *34*, 5627.
- (2) Yu, A. E.; Hu, S.; Spiro, T. G.; Burstyn, J. N. *J. Am. Chem. Soc.* **1994**, *116*, 4117.
- (3) Traylor, T. G.; Sharma, V. S. *Biochemistry* **1992**, *31*, 2847.
- (4) Selected reviews on the biology of NO: (a) *Nitric Oxide: Biochemistry, Molecular Biology, and Therapeutic Implications*; Ignarro, L., Murad, F., Eds.; Advances in Pharmacology 34; Academic: San Diego, CA, 1995. (b) Moncada, S.; Palmer, R. M. J.; Higgs, E. A. *Pharmacol. Rev.* **1991**, *43*, 109. (c) Ignarro, L. J. *Annu. Rev. Pharmacol. Toxicol.* **1990**, *30*, 535.
- (5) (a) Scheidt, W. R.; Frisse, M. E. *J. Am. Chem. Soc.* **1975**, *97*, 17. (b) Mu, X. H.; Kadish, K. M. *Inorg. Chem.* **1988**, *27*, 4720. (c) Choi, I.-K.; Liu, Y.; Feng, D.; Paeng, K.-J.; Ryan, M. D. *Inorg. Chem.* **1991**, *30*, 1832. (d) Yoshimura, T. *Bull. Chem. Soc. Jpn.* **1991**, *64*, 2819. (e) Hoshino, M.; Ozawa, K.; Seki, H.; Ford, P. C. *J. Am. Chem. Soc.* **1993**, *115*, 9568. (f) Lançon, D.; Kadish, K. M. *J. Am. Chem. Soc.* **1983**, *105*, 5610. (g) Wayland, B. B.; Olson, L. W. *J. Am. Chem. Soc.* **1974**, *96*, 6037.
- (6) (a) Bohle, D. S.; Hung, C.-H. *J. Am. Chem. Soc.* **1995**, *117*, 9584. (b) Scheidt, W. R.; Piculio, P. L. *J. Am. Chem. Soc.* **1976**, *98*, 1913. (c) Scheidt, W. R.; Frisse, M. E. *J. Am. Chem. Soc.* **1975**, *97*, 17. (d) Scheidt, W. R.; Brinegar, A. C.; Ferro, E. B.; Kirner, J. F. *J. Am. Chem. Soc.* **1977**, *99*, 7315. (e) Nasri, H.; Haller, K. J.; Wang, Y.; Huynh, B. H.; Scheidt, W. R. *Inorg. Chem.* **1992**, *31*, 3459. (f) Yoshimura, T.; Ozaki, T. *Arch. Biochem. Biophys.* **1984**, *229*, 126. (g) Wayland, B. B.; Olson, L. W. *J. Am. Chem. Soc.* **1974**, *96*, 6037. (h) Waleh, A.; Ho, N.; Chantranupong, L.; Loew, G. H. *J. Am. Chem. Soc.* **1989**, *111*, 2767. (i) Lipscomb, L. A.; Lee, B.-S.; Yu, N.-T. *Inorg. Chem.* **1993**, *32*, 281. (j) Lançon, D.; Kadish, K. M. *J. Am. Chem. Soc.* **1983**, *105*, 5610.
- (7) Richter-Addo, G. B.; Legzdins, P. *Metal Nitrosyls*; Oxford University Press: New York, 1992; Chapters 2 and 6.
- (8) Cheng, S.-H.; Su, Y. O. *Inorg. Chem.* **1994**, *33*, 5847.
- (9) (a) Mochida, I.; Suetsugu, K.; Fujitsu, H.; Takeshita, K. *J. Chem. Soc., Chem. Commun.* **1982**, 166. (b) Tsuji, K.; Imaizumi, M.; Oyoshi, A.; Mochida, I.; Fujitsu, H.; Takeshita, K. *Inorg. Chem.* **1982**, *21*, 721.
- (10) Scheidt, W. R.; Hoard, J. L. *J. Am. Chem. Soc.* **1973**, *95*, 8281.
- (11) (a) Hori, H.; Ikeda-Saito, M.; Leigh, J. S.; Yonetani, T. *Biochemistry* **1982**, *21*, 1431. (b) Yu, N.-T.; Thompson, H. M.; Mizukami, H.; Gersonde, K. *Eur. J. Biochem.* **1986**, *159*, 129.

and co-workers have prepared porphyrin and hydroporphyrin complexes such as (OEP)Co(NO), (OEC)Co(NO), or (OEiBC)-Co(NO) and have spectroscopically characterized their π -cation radical oxidation products (OEP, OEC, and OEiBC are the dianions of octaethylporphyrin, octaethylchlorin, and octaethylisobacteriochlorin, respectively).¹² Importantly, Burstyn has shown that (protoporphyrin-IX)Co(NO) activates soluble guanylate cyclase to a greater extent than do the Fe and Mn analogs.¹³

The upsurge of interest in cobalt nitrosyl porphyrins led us to extend the data available on cobalt nitrosyl porphyrins containing a TPP or OEP macrocycle^{10,12,14} and study how subtle but systematic changes in porphyrin ring basicity might be related to changes in the spectroscopic and electrochemical properties of *structurally related* cobalt nitrosyl porphyrins. This is examined in the present paper for eight different porphyrins of the form (T(*p/m*-X)PP)Co(NO), where X is an electron-donating or electron-withdrawing substituent on the *para* or *meta* positions of the four phenyl rings of the porphyrin. The singly oxidized compounds are also characterized with respect to the site of oxidation and the effect of substituents on their spectroscopic properties. The investigated compounds are represented as (P)Co(NO) and [(P)Co(NO)]⁺ where P is the dianion of a given porphyrin ring.

Experimental Section

All reactions were performed under an atmosphere of prepurified nitrogen using standard Schlenk glassware and/or in an Innovative Technology Labmaster 100 drybox. Solutions for spectral studies were also prepared under a nitrogen atmosphere. Solvents were distilled from appropriate drying agents under nitrogen just prior to use: CH₂Cl₂ (CaH₂), benzene (Na), toluene (Na), ether (Na/benzophenone), THF (Na/benzophenone), hexane (Na/benzophenone/tetraglyme), and acetonitrile (Na). Anhydrous deaerated methanol was purchased from Aldrich Chemical Co. and used as received.

Chemicals. (T(*p*-OCH₃)PP)Co and (TPP)Co were purchased from Aldrich Chemical Co. and used as received. The remaining *para*- and *meta*-substituted tetraphenylporphyrins, T(*p*-X)PPH₂ and T(*m*-X)-PPH₂, were synthesized by condensation of the precursor benzaldehydes and pyrrole using the method of Adler.¹⁵ The corresponding cobalt derivatives, (T(*p*-X)PP)Co and (T(*m*-X)PP)Co, were obtained by refluxing the free-base porphyrins with Co(CH₃CO₂)₂·4H₂O in dimethylformamide.¹⁶ Chloroform-*d* (99.8%, Cambridge Isotope Laboratories) was vacuum-distilled from CaH₂ under nitrogen prior to use. Elemental analyses were performed by Atlantic Microlab, Norcross, GA. Nitric oxide (98%, Matheson Gas) was passed through KOH pellets and a cold trap (dry ice/acetone, -78 °C) to remove higher nitrogen oxides.

Absolute dichloromethane (CH₂Cl₂) over molecular sieves (for electrochemistry) was obtained from Fluka Chemica and used without further purification. Tetra-*n*-butylammonium perchlorate (TBAP) and tetra-*n*-butylammonium hexafluorophosphate (TBAH) were purchased from Fluka Chemica. TBAP and TBAH were recrystallized from ethyl alcohol and ethyl acetate, respectively. Both salts, used as supporting electrolytes, were dried under vacuum at 40 °C for at least 1 week prior

to use. Nitrogen of "ultrahigh-purity grade" for electrochemistry was purchased from Trigas (Houston, TX).

Instrumentation. Infrared spectra were recorded on a Bio-Rad FT-155 FTIR spectrometer or a Nicolet Magna-IR 550 FTIR spectrometer with a resolution of 2–4 cm⁻¹. Proton NMR spectra were obtained on a Varian XL-300 spectrometer and the signals referenced to the residual signal of the solvent employed (CDCl₃). All couplings are in hertz. FAB mass spectra were obtained on a VG-ZAB-E mass spectrometer. UV–vis spectra were recorded on a Hewlett Packard Model 8452A diode array instrument.

Cyclic voltammetry was carried out with an EG&G Model 173 potentiostat or an IBM Model EC 225 voltammetric analyzer. Current–voltage curves were recorded on an EG&G Princeton Applied Research Model RE-0151 X-Y recorder. A three-electrode system was used and consisted of a platinum button working electrode, a platinum wire counter electrode, and a saturated calomel reference electrode (SCE). The reference electrode was separated from the bulk of the solution by a fritted-glass bridge filled with the solvent/supporting electrolyte mixture. Low-temperature measurements were performed by placing the electrochemical cell in an acetone bath which was cooled at the desired temperature by addition of dry ice. All potentials are reported versus the SCE.

Thin-layer controlled-potential electrolyses were carried out with an EG&G Model 173 potentiostat, and current–time curves were recorded on an EG&G Princeton Applied Research Model RE-0151 X-Y recorder. The design of the thin-layer cell has been described elsewhere.¹⁷

Infrared spectroelectrochemical measurements were carried out with a Nicolet Magna-IR 550 FTIR spectrometer. The design of the thin-layer spectroelectrochemical cell is described in the literature.¹⁸ All spectra were collected under a nitrogen atmosphere, and multiple scans were taken over the desired frequency region in order to improve the signal-to-noise ratio. Potentials for oxidation of each compound were applied and monitored with an EG&G Model 173 potentiostat. The concentration of each porphyrin was approximately 1 mM, while that of the supporting electrolyte, which does not interfere in the investigated spectral region (1500–1900 cm⁻¹), was 0.2 M. Thin-layer cyclic voltammograms were recorded in the spectroelectrochemical cell prior to IR measurements in order to determine the stability of the electrogenerated product. At the same time, the values of *E*_{1/2} under these conditions were used in order to evaluate the appropriate potentials for generating a given electrooxidized species in the thin-layer cell.

Synthesis of (T(*p*-X)PP)Co(NO) and (T(*m*-X)PP)Co(NO). The investigated compounds were synthesized by three different methods. The first two (methods A and B) involve a reaction of the precursor (P)Co complexes with NO, while the third (method C) involves formation of [(P)Co(NO)]⁺ followed by chemical reduction with cobaltocene to give (P)Co(NO). The synthesis of (T(*p*-OCH₃)PP)Co(NO) is described as a representative example for methods A and B, while method C is presented in a later section under the synthesis of [(P)Co(NO)]BF₄. **Caution:** Nitric oxide is toxic, and reactions should be performed in a well-vented fume hood.

Method A. A Schlenk flask was charged with (T(*p*-OCH₃)PP)Co (0.200 g, 0.253 mmol) and CH₂Cl₂ (20 mL). The mixture was stirred to generate a purple solution, and NO gas was then bubbled through the solution for 20 min. During this time, the color of the reaction mixture turned red-purple. The solution was then heated to boiling and the volume reduced in vacuo to ca. 5 mL. Anhydrous deaerated CH₃OH (5 mL) was added, which led to precipitation of a purple solid. The supernatant solution was discarded by careful removal with a syringe, and the solid was dried in vacuo. The solid was then recrystallized from toluene/hexane (10:1) to give (T(*p*-OCH₃)PP)Co(NO) (0.150 g, 0.183 mmol, 72% yield).

Method B. A Schlenk flask was charged with (T(*p*-OCH₃)PP)Co (0.316 g, 0.399 mmol), CH₂Cl₂ (55 mL), and piperidine (1.5 mL). The mixture was stirred to generate a purple solution, and NO gas was bubbled through the solution for 30 min. During this time, the color of the reaction mixture turned red-purple. Nitrogen was then bubbled through the solution for 2 min to remove any unreacted NO. The

- (12) (a) Fujita, E.; Chang, C. K.; Fajer, J. *J. Am. Chem. Soc.* **1985**, *107*, 7665. (b) Fujita, E.; Fajer, J. *J. Am. Chem. Soc.* **1983**, *105*, 6743.
- (13) (a) Burstyn, J. N. In *Abstracts of Papers*, 210th National Meeting of the American Chemical Society, Chicago, IL; American Chemical Society: Washington, DC, 1995; INOR 254. (b) Reynolds, M. F.; Graham, J. P.; Dierks, E. A.; Burstyn, J. N.; Bursten, B. E. *Ibid.*, INOR 095.
- (14) (a) Wayland, B. B.; Minkiewicz, J. V.; Abd-Elmageed, M. E. *J. Am. Chem. Soc.* **1974**, *96*, 2795. (b) Groombridge, C. J.; Larkworthy, L. F.; Mason, J. *Inorg. Chem.* **1993**, *32*, 379.
- (15) Adler, A. D.; Longo, F. R.; Finarelli, J. D.; Goldmacher, J.; Assour, J.; Korsakoff, L. *J. Org. Chem.* **1967**, *32*, 476.
- (16) Adler, A. D.; Longo, F. R.; Kampas, F.; Kim, J. *J. Inorg. Nucl. Chem.* **1970**, *32*, 2443.

- (17) Lin, X. Q.; Kadish, K. M. *Anal. Chem.* **1985**, *57*, 1498.

- (18) Lin, X. Q.; Mu, X. H.; Kadish, K. M. *Electroanalysis* **1989**, *1*, 35.

solution was heated to boiling and CH₃OH (150 mL) added to precipitate a purple solid. The solution was allowed to cool to room temperature and the microcrystalline solid collected by filtration on a medium-porosity frit. This solid was then washed with CH₃OH (30 mL), recrystallized from CH₂Cl₂/hexane (*ca.* 30 mL, 1:1), and dried under vacuum to give (T(*p*-OCH₃)PP)Co(NO) (0.208 g, 0.253 mmol, 63% yield).

The other complexes were obtained by both methods.

(T(*p*-OCH₃)PP)Co(NO) (1). Anal. Calcd for C₄₈H₃₆N₅O₅Co: C, 70.16; H, 4.42; N, 8.52. Found: C, 70.26; H, 4.50; N, 8.43. Low-resolution mass spectrum (FAB): *m/z* 791 [(T(*p*-OCH₃)PP)Co]⁺. IR (KBr; cm⁻¹): ν_{NO} 1679 s; also 1607 m, 1547 vw, 1507 s, 1462 w, 1441 w, 1351 m, 1249 vs, 1173 s, 1106 w, 1002 s, 801 m br. IR (CH₂Cl₂; cm⁻¹): ν_{NO} 1682. ¹H NMR (CDCl₃; δ, ppm): 8.91 (s, 8 H, pyrrole H), 7.25 (d, *J* = 8, 8 H, *m*-H), 8.06 (d, *J* = 8, 8 H, *o*-H), 4.06 (s, 12 H, OCH₃). UV-vis (CH₂Cl₂; λ, nm (10⁻⁵ε)): 540 (1.31), 420 (12.12).

(T(*p*-CH₃)PP)Co(NO) (2). Yields: method A, 68%; method B, 67%. Anal. Calcd for C₄₈H₃₆N₅OCo: C, 76.08; H, 4.79; N, 9.24. Found: C, 75.51; H, 4.83; N, 9.06. Low-resolution mass spectrum (FAB): *m/z* 727 [(T(*p*-CH₃)PP)Co]⁺. IR (KBr; cm⁻¹): ν_{NO} 1678 s; also 1597 m, 1508 w, 1451 w, 1351 m, 1109 w, 1005 s, 799 s. IR (CH₂Cl₂; cm⁻¹): ν_{NO} 1681. ¹H NMR (CDCl₃; δ, ppm): 8.90 (s, 8 H, pyrrole H), 7.51 (d, *J* = 8, 8 H, *m*-H), 8.03 (d, *J* = 8, 8 H, *o*-H), 2.66 (s, 12 H, CH₃). UV-vis (CH₂Cl₂; λ, nm (10⁻⁵ε)): 540 (1.50), 416 (10.85).

(T(*m*-CH₃)PP)Co(NO) (3). Yields: method A, 85%; method B, 54%. Anal. Calcd for C₄₈H₃₆N₅OCo: C, 76.08; H, 4.79; N, 9.24. Found: C, 75.87; H, 4.82; N, 9.12. Low-resolution mass spectrum (EI): *m/z* 727 [(T(*m*-CH₃)PP)Co]⁺. IR (KBr; cm⁻¹): ν_{NO} 1681 s; also 1604 m, 1548 vw, 1452 w, 1004 m, 797 m. IR (CH₂Cl₂; cm⁻¹): ν_{NO} 1682. ¹H NMR (CDCl₃; δ, ppm): 8.91 (s, 8 H, pyrrole H), 7.98 (d, *J* = 8, 4 H, *o'*-H), 7.97 (s, 4 H, *o*-H), 7.60 (dd, *J* = 8/8, 4 H, *m*-H), 7.54 (d, *J* = 8, 4 H, *p*-H), 2.60 (s, 12 H, CH₃). UV-vis (CH₂Cl₂; λ, nm (10⁻⁵ε)): 536 (2.01), 414 (13.84).

(TPP)Co(NO) (4).¹⁰ Yields: method A, 71%; method B, 84%. Low-resolution mass spectrum (FAB): *m/z* 671 [(TPP)Co]⁺. IR (KBr; cm⁻¹): ν_{NO} 1693 s; also 1592 m, 1438 w, 1345 s, 1168 s, 1068 m, 995 s, 798 s. IR (CH₂Cl₂; cm⁻¹): ν_{NO} 1683. ¹H NMR (CDCl₃; δ, ppm): 8.89 (s, 8H, pyrrole H), 7.72 (d (app), *J* = 8, 12H, *m*-H and *p*-H), 8.15 (d, *J* = 8, 8H, *o*-H). UV-vis (CH₂Cl₂; λ, nm (10⁻⁵ε)): 536 (2.51), 414 (17.70).

(T(*m*-OCH₃)PP)Co(NO) (5). Yields: method A, 43%; method B, 79%. Anal. Calcd for C₄₈H₃₆N₅O₅Co: C, 70.16; H, 4.42; N, 8.52. Found: C, 69.88; H, 4.51; N, 8.40. Low-resolution mass spectrum (FAB): *m/z* 791 [(T(*m*-OCH₃)PP)Co]⁺. IR (KBr; cm⁻¹): ν_{NO} 1677 s; also 1581 s, 1458 s, 1424 s, 1347 m, 1278 m, 1167 s, 1003 s, 796 s. IR (CH₂Cl₂; cm⁻¹): ν_{NO} 1682. ¹H NMR (CDCl₃; δ, ppm): 8.94 (s, 8 H, pyrrole H), 7.76 (d, *J* = 7, 4 H, *o'*-H), 7.71 (s, 4 H, *o*-H), 7.62 (dd, *J* = 7/8, 4 H, *m*-H), 7.30 (d, *J* = 8, 4 H, *p*-H), 3.96 (s, 12 H, OCH₃). UV-vis (CH₂Cl₂; λ, nm (10⁻⁵ε)): 536 (1.78), 414 (13.93).

(T(*p*-OCF₃)PP)Co(NO) (6). Yields: method A, 56%; method B, 54%. Anal. Calcd for C₄₈H₂₄N₅O₃F₁₂Co: C, 55.56; H, 2.33; N, 6.75. Found: C, 55.49; H, 2.36; N, 6.69. Low-resolution mass spectrum (FAB): *m/z* 1007 [(T(*p*-OCF₃)PP)Co]⁺. IR (KBr; cm⁻¹): ν_{NO} 1696 s; also 1608 w, 1544 w, 1502 m, 1457 w, 1351 m, 1278 m, 1166 s, 1100 w, 1005 s, 825 m, 796 s. IR (CH₂Cl₂; cm⁻¹): ν_{NO} 1685. ¹H NMR (CDCl₃; δ, ppm): 8.88 (s, 8H, pyrrole H), 7.60 (d, *J* = 8, 8H, *m*-H), 8.17 (d, *J* = 8, 8H, *o*-H). UV-vis (CH₂Cl₂; λ, nm (10⁻⁵ε)): 536 (1.77), 412 (14.77).

(T(*p*-CF₃)PP)Co(NO) (7). Yields: method A, 63%; method B, 30%. Anal. Calcd for C₄₈H₂₄N₅O₂F₁₂Co: C, 59.21; H, 2.48; N, 7.19. Found: C, 59.20; H, 2.52; N, 7.16. Low-resolution mass spectrum (FAB): *m/z* 943 [(T(*p*-CF₃)PP)Co]⁺. IR (KBr; cm⁻¹): ν_{NO} 1691 s; also 1617 m, 1404 w, 1324 vs, 1166 s, 1107 m, 1003 m, 816 m, 798 w. IR (CH₂Cl₂; cm⁻¹): ν_{NO} 1690. ¹H NMR (CDCl₃; δ, ppm): 8.85 (s, 8H, pyrrole H), 8.01 (d, *J* = 8, 8H, *m*-H), 8.28 (d, *J* = 8, 8H, *o*-H). UV-vis (CH₂Cl₂; λ, nm (10⁻⁵ε)): 536 (1.76), 410 (14.10).

(T(*p*-CN)PP)Co(NO) (8). Yields: method A, 55%; method B, 49%. Anal. Calcd for C₄₈H₂₄N₉OCo: C, 71.91; H, 3.08; N, 15.72. Found: C, 71.85; H, 3.08; N, 15.67. Low-resolution mass spectrum (FAB): *m/z* 771 [(T(*p*-CN)PP)Co]⁺. IR (KBr; cm⁻¹): ν_{NO} 1684 s; also 1606

m, 1545 w, 1500 w, 1399 w, 1351 m, 1107 w, 1002 s, 812 s, 799 m. IR (CH₂Cl₂; cm⁻¹): ν_{NO} 1695. ¹H NMR (CDCl₃; δ, ppm): 8.84 (s, 8H, pyrrole H), 7.60 (d, *J* = 8, 8H, *m*-H), 8.06 (d, *J* = 8, 8H, *o*-H). UV-vis (CH₂Cl₂; λ, nm (10⁻⁵ε)): 538 (1.55), 412 (11.50).

Alternate Preparation Method for (T(*p*-OCH₃)PP)Co(NO). To a stirred CH₂Cl₂ (30 mL) solution of (T(*p*-OCH₃)PP)Co (0.240 g, 0.303 mmol) was added the C₅H₁₀NH₂⁺C₅H₁₀NN₂O₂⁻ salt (0.140 g, 0.609 mmol).¹⁹ The solution was stirred for 30 min, during which the mixture turned from red to red purple. The solution was then heated to boiling, after which CH₃OH (100 mL) was added to precipitate a purple solid. The solution was allowed to cool to room temperature, and the microcrystalline solid was collected by filtration on a medium-porosity frit. This solid was then washed with MeOH (20 mL) and dried under vacuum to give (T(*p*-OCH₃)PP)Co(NO) (0.150 g, 0.183 mmol, 60%).

Synthesis of [(T(*p*-X)PP)Co(NO)]BF₄ and [(T(*m*-X)PP)Co(NO)]-BF₄. Two methods were utilized for synthesis of the oxidized derivatives, after which the cationic compounds were reduced by cobaltocene to give (P)Co(NO). The latter manipulation also provides a third method (method C) for preparation of the neutral compounds. The following examples are representative:

Method I (X ≠ OCF₃, CF₃, CN). To a stirred CH₂Cl₂ solution (10 mL) of (T(*p*-OCH₃)PP)Co(NO) (0.061 g, 0.078 mmol) was added AgBF₄ (0.016 g, 0.080 mmol). The solution was stirred for *ca.* 5 min, and an aliquot was then transferred under nitrogen into a sealed NaCl IR cell *via* a cannula.

Method II (X ≠ CN). To a stirred CDCl₃ solution (10 mL) of (T(*m*-CH₃)PP)Co (0.131 g, 0.180 mmol) was added NOBF₄ (0.031 g, 0.265 mmol). The solution was stirred for *ca.* 5 min, and an aliquot was then transferred under nitrogen into the sealed IR cell *via* a cannula.

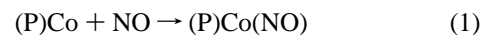
Attempts to generate [(T(*p*-CN)PP)Co(NO)]BF₄ from either method I or method II resulted in the immediate formation of a highly insoluble product that was not further characterized.

Chemical Reduction of Oxidized Compounds (Method C). Green solutions of [(T(*p*-X)PP)Co(NO)]BF₄ and [(T(*m*-X)PP)Co(NO)]BF₄ (X ≠ CN; generated by method II above) were reacted with 1 equiv of cobaltocene to generate the neutral (P)Co(NO) complexes in 32–67% isolated yields (**1** (40%), **2** (32%), **3** (39%), **4** (35%), **5** (44%), **6** (67%), **7** (64%, from CH₂Cl₂)).

Structural Determination of (T(*p*-OCH₃)PP)Co(NO) (1). A crystal of (T(*p*-OCH₃)PP)Co(NO) was grown from a CH₂Cl₂/CH₃OH solution (*ca.* 1:1) kept at -20 °C for 2 weeks. X-ray data were collected at 228(2) K on an Enraf Nonius CAD-4 diffractometer using monochromated Mo Kα radiation (λ = 0.710 73 Å). Data were corrected for Lorentz and polarization effects. No absorption correction was applied since it was judged to be insignificant. The structure was solved using the SHELXTL (Siemens) system and refined by full-matrix least-squares methods on *F*² for all reflections. Weighted *R* factors, wR₂, and goodness of fit are based on *F*². Details of crystal data and refinement are given in Table 1, atomic coordinates and equivalent isotropic displacement parameters are given in Table 2, and selected bond lengths and angles are collected in Table 3.

Results and Discussion

Nitric oxide reacts directly with the readily synthesizable four-coordinate (P)Co compounds in CH₂Cl₂ at room temperature to produce the corresponding five-coordinate (P)Co(NO) complexes in 43–85% yields (eq 1) depending upon the specific phenyl ring substituents.



During the course of addition of NO gas (usually 10–20 min), the color of the reaction mixture changes from purple to red-purple. However, all of the (P)Co(NO) compounds are purple in the solid state, except the *p*-CN derivative, which is red-purple. These five-coordinate complexes are moderately stable in air in the solid state, showing no noticeable signs of decomposition over a 2–3 week period, as judged by their IR and ¹H NMR spectra. The parent (TPP)Co(NO) was previously

Table 1. Crystal Data and Structure Refinement Details for (T(*p*-OCH₃)PP)Co(NO) (**1**)

formula	C ₄₈ H ₃₆ CoN ₅ O ₅
fw	821.75
<i>T</i> , K	228(2)
<i>λ</i> , Å	0.71073
crystal system	monoclinic
space group	<i>P</i> 2/ <i>c</i>
unit cell dimensions	<i>a</i> = 15.052(1) Å, <i>b</i> = 9.390(1) Å, <i>c</i> = 16.274(2) Å, α = 90°, β = 111.04(1)°, γ = 90°
<i>V</i> , Å ³	2146.8(4)
<i>Z</i>	2
<i>D</i> (calcd), g/cm ³	1.271
abs coeff, mm ⁻¹	0.451
<i>F</i> (000)	852
crystal size	0.4 × 0.3 × 0.2 mm
θ range for data collection	2.17–26.56°
index ranges	−17 ≤ <i>h</i> ≤ 16, 0 ≤ <i>k</i> ≤ 11, −1 ≤ <i>l</i> ≤ 16
no. of rflns collected	3507
no. of independent rflns	3348
refinement method	full-matrix least-squares on <i>F</i> ²
data/parameters	3330/275
goodness-of-fit on <i>F</i> ²	1.054
final <i>R</i> indices [<i>I</i> > 2σ(<i>I</i>)] ^{a,b}	<i>R</i> 1 = 0.0599, <i>wR</i> 2 = 0.1567
<i>R</i> indices (all data) ^{a,b}	<i>R</i> 1 = 0.0904, <i>wR</i> 2 = 0.2009
largest diff peak and hole	0.842 and −0.281 e Å ⁻³

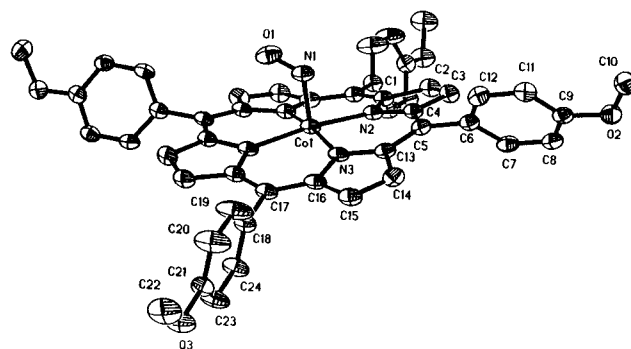
$$^a R1 = \sum ||F_o| - |F_c|| / \sum |F_o|, \quad ^b wR2 = \{ \sum [w(F_o^2 - F_c^2)^2] / \sum [wF_o^4] \}^{1/2}.$$

Table 2. Atomic Coordinates (×10⁴) and Equivalent Isotropic Displacement Parameters (Å² × 10³) for (T(*p*-OCH₃)PP)Co(NO)

	<i>x</i>	<i>y</i>	<i>z</i>	<i>U</i> _{eq} ^a
Co(1)	0	2255(1)	2500	45(1)
O(1)	−232(5)	4859(8)	3029(5)	76(2)
O(2)	2017(2)	3204(3)	−2333(2)	61(1)
O(3)	5530(2)	479(4)	6652(3)	83(1)
N(1)	0	4230(6)	2500	55(2)
N(2)	−576(2)	2106(3)	1102(2)	44(1)
N(3)	1155(2)	2042(3)	2369(2)	45(1)
C(1)	−1463(3)	1942(4)	578(3)	49(1)
C(2)	−1610(3)	2065(5)	−409(3)	58(1)
C(3)	−836(3)	2344(5)	−499(3)	56(1)
C(4)	−185(3)	2316(4)	448(3)	46(1)
C(5)	717(3)	2390(4)	635(3)	46(1)
C(6)	1041(3)	2639(4)	−158(3)	48(1)
C(7)	935(3)	1633(5)	−877(3)	54(1)
C(8)	1258(3)	1850(5)	−1579(3)	55(1)
C(9)	1708(3)	3088(5)	−1608(3)	51(1)
C(10)	2406(4)	4524(6)	−2437(4)	79(2)
C(11)	1811(3)	4115(5)	−919(3)	57(1)
C(12)	1476(3)	3874(5)	−209(3)	57(1)
C(13)	1332(3)	2149(4)	1551(3)	48(1)
C(14)	2255(3)	1934(5)	1746(3)	58(1)
C(15)	2632(3)	1691(5)	2676(4)	60(1)
C(16)	1964(3)	1791(4)	3088(3)	49(1)
C(17)	2114(3)	1732(5)	4038(3)	49(1)
C(18)	3032(3)	1429(5)	4726(3)	52(1)
C(19)	3662(4)	2479(6)	5010(5)	104(3)
C(20)	4505(4)	2197(6)	5662(5)	100(2)
C(21)	4718(3)	865(5)	6011(3)	59(1)
C(22)	6178(4)	1537(7)	6986(5)	100(2)
C(23)	4111(3)	−201(6)	5719(4)	77(2)
C(24)	3278(3)	94(5)	5080(4)	66(2)

^a Equivalent isotropic *U* is defined as one-third of the trace of the orthogonalized *U*_{ij} tensor.

synthesized by Scheidt via reaction of (TPP)Co with NO in the presence of piperidine¹⁰ and by Wayland in the absence of base.^{14a} We repeated the syntheses of each cobalt nitrosyl complex in the presence of piperidine and, consistent with the observation by Scheidt, also obtained the desired compounds (containing no piperidine axial ligand) in 30–79% yields. In

**Figure 1.** Molecular structure of (T(*p*-OCH₃)PP)Co(NO). Only one of the two disordered positions of the nitrosyl O1 atom is shown. Hydrogen atoms have been omitted for clarity.

the latter instance, a nitric oxide–amine adduct of the form (R₂NH₂)⁺[R₂NN(O)NO][−] is the source of NO for metal–nitrosyl formation.²⁰ The reaction of (T(*p*-OCH₃)PP)Co with authentic (R₂NH₂)⁺[R₂NN(O)NO][−] (R₂ = C₅H₁₀), derived from the reaction of piperidine with nitric oxide,¹⁹ resulted (after workup) in the isolation of **1** in 60% yield. Compounds **1**–**7** could also be generated in CH₂Cl₂ by reaction of the respective (P)Co derivatives with NO⁺, followed by reduction with cobaltocene (see following section).

In CH₂Cl₂, the IR spectra of the neutral porphyrins show a strong band in the 1681–1695 cm^{−1} region which is assignable to ν_{NO}.⁷ These values are similar to those reported previously for (TPP)Co(NO) (1689 cm^{−1}, KBr)^{10,14} and (OEP)Co(NO) (1675 cm^{−1}, CH₂Cl₂)^{12,14} and are close to the range of NO frequencies reported for square pyramidal N-substituted salicylideamine complexes of cobalt containing a bent NO ligand (1645–1675 cm^{−1}, Nujol mull).²¹ Low-resolution mass spectra of the (P)Co(NO) complexes are dominated by peaks assignable to the [(P)Co]⁺ fragments, a feature consistent with the facile loss of the NO axial ligand under our measurement conditions.

In CDCl₃, the ambient-temperature ¹H NMR spectra of all eight (P)Co(NO) complexes consist of sharp peaks, which indicates that each compound is diamagnetic. This diamagnetism was confirmed by solution measurements of the magnetic moment using the Evans method.²² All of the complexes display pyrrole H resonances in the 8.84–8.94 ppm region. Furthermore, the ¹H NMR spectra of the *para*-substituted complexes show a doublet for the *ortho* and *meta* protons of the substituted phenyl ring, a feature that suggests a rapid rotation of the phenyl rings on the NMR time scale.²³

The molecular structure of (T(*p*-OMe)PP)Co(NO) (**1**) is shown in Figure 1, and selected bond lengths and angles are shown in Table 3. The molecule is situated at the crystallographic 2-fold center, and only half is unique. The Co(1) and N(1) atoms lie on the 2-fold axis, and the nitrosyl O(1) atom is disordered at two sites.

The most notable feature of the structure is that the Co–N–O group is bent and has a bond angle of 119.6(4)°. The NO ligand is oriented between two adjacent porphyrin nitrogens, as shown in Figure 2a, and a similar feature is observed for the related five-coordinate (P)Fe(NO) compounds.^{6a} Nevertheless, the structural observation of a bent NO ligand is consistent with

(20) Piccolo, P. L.; Scheidt, W. R. *Inorg. Nucl. Chem. Lett.* **1975**, *11*, 309.

(21) Groombridge, C. J.; Larkworthy, L. F.; Marecaux, A.; Povey, D. C.; Smith, G. W.; Mason, J. J. *Chem. Soc., Dalton Trans.* **1992**, 3125.

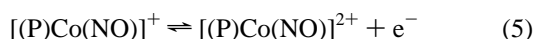
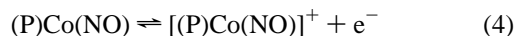
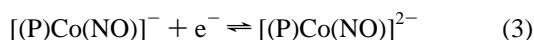
(22) Grant, D. H. J. *Chem. Educ.* **1995**, *72*, 39 and references therein.

(23) (a) Eaton, S. S.; Fishwild, D. M.; Eaton, G. R. *Inorg. Chem.* **1978**, *17*, 1542. (b) Eaton, S. S.; Eaton, G. R. *J. Am. Chem. Soc.* **1977**, *99*, 6594.

Table 4. Half-Wave Potentials (V vs SCE) for Oxidations and Reductions of (T(*p*/*m*-X)PP)Co(NO)^a in CH₂Cl₂, 0.2 M TBAP and TBAH

compd no.	X	σ^b	$E_{1/2}$							
			1st oxidn		2nd oxidn		1st redn		2nd redn ^c	
			TBAP	TBAH	TBAP	TBAH	TBAP	TBAH	TBAH	
1	<i>p</i> -OCH ₃	-0.27	0.93	0.89	1.19	1.23	-1.20	-1.20	-1.78	
2	<i>p</i> -CH ₃	-0.17	0.97	0.91	1.23	1.27	-1.19	-1.20	-1.75	
3	<i>m</i> -CH ₃	-0.07	0.98	0.93	1.23	1.28	-1.20	-1.18	-1.74	
4	H	0.00	1.01	0.96	1.20	1.27	-1.18	-1.16	-1.73	
5	<i>m</i> -OCH ₃	0.12	1.01	0.97	1.23	1.20 ^c	-1.18	-1.15	-1.72	
6	<i>p</i> -OCF ₃	0.35	1.11	1.06		1.32	-1.12	-1.10	-1.63	
7	<i>p</i> -CF ₃	0.55	1.15	1.14		1.34 ^c	-1.10	-1.06	-1.55	
8	<i>p</i> -CN	0.63	1.20	1.15		1.37	-1.02	-1.05	-1.50	

^a X is a given substituent on each meso phenyl. ^b Hammett parameters taken from ref 23. ^c Potentials were determined at -60 °C.



are shown in Figure 3. The two oxidations are well-defined for six of the eight compounds (i.e. compounds 1–6) at room temperature, the exceptions being (T(*p*-CF₃)PP)Co(NO) (7) and (T(*p*-CN)PP)Co(NO) (8). Both the first and second oxidations of 7 become reversible at -60 °C, but this is not the case for 8, where the singly oxidized product adsorbs at the electrode surface, leading to a first oxidation process having an ill-defined current–voltage curve. The separation in peak potentials, $\Delta E_p = |E_{pa} - E_{pc}|$, ranges from 60 to 70 mV for the first oxidation of each investigated compound and from 60 to 120 mV for the second oxidation, the only exception being those of (T(*p*-CN)-PP)Co(NO), which has an irreversible first oxidation. All of the other compounds have an anodic to cathodic peak current ratio, i_{pa}/i_{pc} , of ≈ 1.0 for both the first and second oxidations. The overall electrochemical data thus suggest that the two oxidations of compounds 1–7 involve diffusion-controlled reversible to quasi-reversible one-electron transfers.

Half-wave potentials for oxidation and reduction of each compound in CH₂Cl₂ containing either TBAH or TBAP are given in Table 4, which also lists the Hammett σ parameters²⁷ associated with each substituent on the *para* or *meta* positions of the four phenyl rings of the porphyrin. The changes in $E_{1/2}$ as a function of substituent are as expected on the basis of linear free energy relationships; i.e., those compounds with electron-donating substituents are easier to oxidize and harder to reduce than (TPP)Co(NO) ($\sigma = 0$), while those with electron-withdrawing substituents show an opposite effect.

The electrochemistry of metalloporphyrins in nonaqueous media has been reviewed.²⁸ For each of the eight compounds in Table 4, the $\Delta E_{1/2}$ between the first and second oxidation falls in the range 220–340 mV, a value that is much smaller than the $\Delta E_{1/2}$ between the first and the second reductions, which ranges from 450 to 580 mV. A similar result has been reported for the redox reactions of (T(*p*-X)PP)Co²⁹ and was explained by a difference in the site of electron transfer; i.e., both the second and third oxidations of (T(*p*-X)PP)Co were assigned as being ring-centered processes, while their first reductions were assigned as being metal-centered, i.e. Co(II)/Co(I) reactions.²⁹

As also seen in Table 4, the $\Delta E_{1/2}$ between the first and second oxidations of most of the eight compounds is larger when

(a) Oxidation at room temperature

(b) Reduction at -60°C

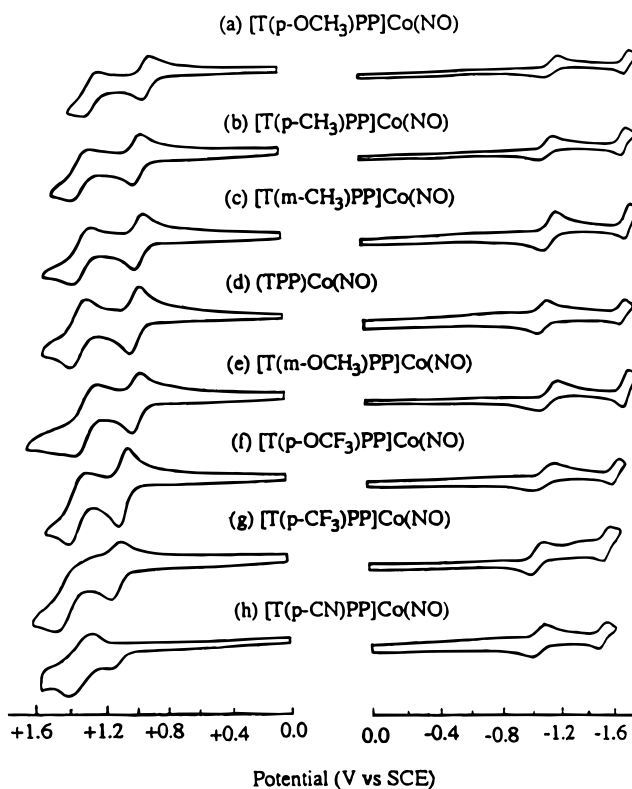


Figure 3. Cyclic voltammograms showing (a) the room-temperature oxidations and (b) low-temperature reductions of each (P)Co(NO) derivative in CH₂Cl₂, 0.2 M TBAH. Scan rate = 0.1 V/s.

TBAH rather than TBAP is used as a supporting electrolyte. This suggests that the singly oxidized product of a given (P)-Co(NO) porphyrin is more stable in the presence of a weakly coordinating counteranion. The same effect has been noted for oxidation of several Ni(II) tetraphenylporphyrins and chlorins.³⁰

In general, substituent effects on redox potentials are larger for porphyrin-ring reactions than for metal-centered reactions in the case of planar TPP-type macrocycles.²⁸ Figure 4 shows plots of $E_{1/2}$ vs the sum of the Hammett parameters (4σ), for each electrode reaction of the compounds. Linear relationships are obtained for the first reduction ($\rho = 44$ mV), as well as the first ($\rho = 76$ mV) and second oxidations ($\rho = 34$ mV) of the compounds. These substituent effects on $E_{1/2}$ can be compared to those reported for the same types of electrode reactions involving substituted cobalt(II) tetraphenylporphyrins not con-

(27) (a) Hansch, C.; Leo, A.; Taft, R. W. *Chem. Rev.* **1991**, *91*, 165. (b) Zuman, P. *Substituent Effects in Organic Polarography*; Plenum: New York, 1967.

(28) Kadish, K. M. *Prog. Inorg. Chem.* **1986**, *34*, 435.

(29) Walker, F. A.; Beroiz, D.; Kadish, K. M. *J. Am. Chem. Soc.* **1976**, *98*, 3484.

(30) Chang, D.; Malinski, T.; Ulman, A.; Kadish, K. M. *Inorg. Chem.* **1984**, *23*, 817.

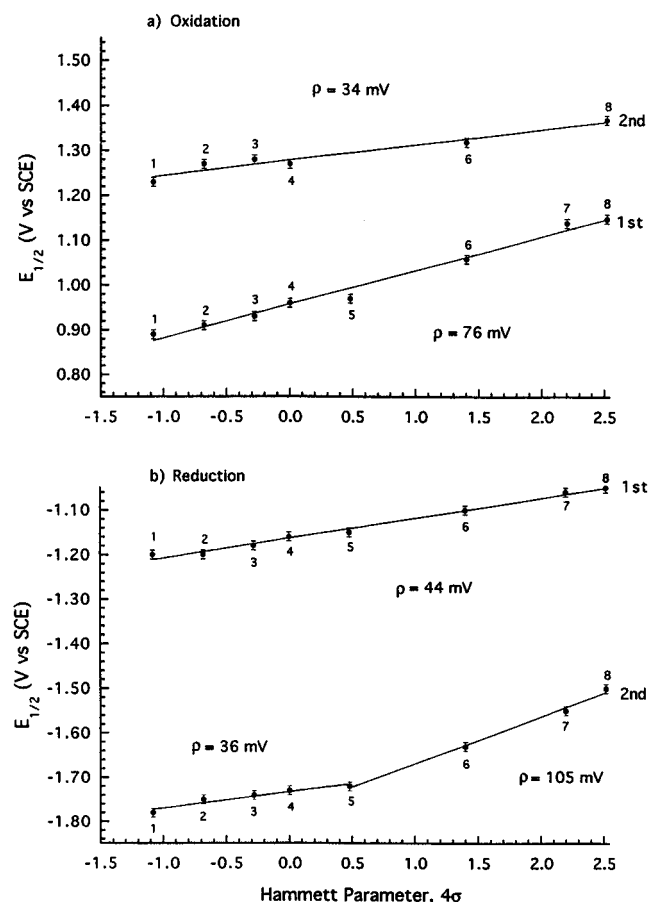
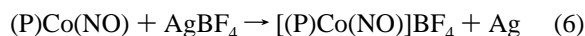


Figure 4. Plot of $E_{1/2}$ vs the Hammett substituent constants for each electrode reaction of (P)Co(NO) in CH_2Cl_2 , 0.1 M TBAH. The compound numbers and half-wave potentials are listed in Table 4.

taining a nitrosyl axial ligand.²⁹ Specifically, a ρ of 41 mV was observed in the plot of $E_{1/2}$ vs 4σ for the first metal-centered reduction of (T(*p*-X)PP)Co, while a ρ of 76 mV was determined for the second ring-centered oxidation of the same series of compounds. A comparison of the ρ values thus indicates that the first oxidation of (P)Co(NO) is ring-centered while the first reduction is proposed to involve the central metal or the nitrosyl axial ligand. The first oxidation of (T(*p*-X)PP)Co was shown to have a $\rho = 34$ mV,²⁹ and this “reduced” substituent effect on $E_{1/2}$ is consistent with the site of electron transfer being the metal center (as opposed to the conjugated π ring system of the macrocycle) in these non-nitrosyl compounds. Although an identical slope is observed for the second oxidation of (P)Co(NO) (Figure 4a), we cannot rule out that this latter electrode reaction involves the NO ligand rather than the cobalt center.

The correlation in Figure 4 between half-wave potentials and 4σ for the second reduction of (P)Co(NO) was made by utilizing data obtained at -60°C and consists of two separate linear segments, one of which has a ρ of 36 mV and the other a ρ of 105 mV. Such a nonlinearity in this correlation is consistent with a change of mechanism which might involve differences in the site of electron transfer^{27b} upon going from compounds 1–5 to compounds 6–8. However, confirmation of this could not be obtained due to the difficulty in stabilizing the doubly reduced species for spectroscopic characterization at -60°C .

Chemical Oxidation. Compounds 1–5 are readily oxidized at room temperature by AgBF_4 to give the corresponding green, air-sensitive [(P)Co(NO)] BF_4 cations.³¹



Although we were not able to obtain the oxidized products in an elementally pure form, these species could be characterized by IR spectroscopy. As seen in Table 5, each chemically oxidized species displays an NO stretching frequency which is about 42 cm^{-1} higher in energy than that of its neutral precursor. Not surprisingly, the cobalt porphyrins with electron-withdrawing substituents on the macrocycle (complexes 6 and 7) are not oxidized by AgBF_4 . The cyano derivative, 8, reacts with Ag^+ , but this results in an immediate precipitation of a highly-insoluble and as yet uncharacterized pink solid ($\nu_{\text{NO}} = 1653\text{ cm}^{-1}$ in Nujol), leaving a colorless supernate. Thus, a subtle change in electronic effect of the peripheral phenyl substituents brings about a marked difference in the oxidation chemistry of the structurally related (P)Co(NO) porphyrins.

Interestingly, we have also been able to generate the cations of (P)Co(NO) by reaction of the precursor (P)Co complexes with NOBF_4 . In general, 1–1.5 equiv of NOBF_4 is needed for the reaction to proceed to completion. These cationic complexes (generated chemically) exhibit ν_{NO} bands that are similar to those of the cationic complexes generated electrochemically (see Table 5). In any event, further reaction of the cations with 1 equiv of the one-electron reducing agent, Cp_2Co , generates the neutral complexes in 32–67% isolated yields (eq 7).



The relatively small shift in ν_{NO} upon conversion of (P)Co(NO) to $[(\text{P})\text{Co}(\text{NO})]^+$ is consistent with oxidation of the complex involving the conjugated π ring system of the macrocycle rather than the metal center. In comparison, shifts of ν_{NO} as high as 170 cm^{-1} are obtained for the metal-centered oxidation of (TPP)Fe(NO).^{5b} In CDCl_3 , the IR spectra of the cationic complexes are also consistent with formation of species which are oxidized at the macrocycle since they show bands in the $1289\text{--}1294\text{ cm}^{-1}$ region that are characteristic of π -cation radicals for TPP-type complexes.³⁴ These marker bands are described as pyrrole half-stretching vibrations.³⁵ Due to the solvent background, these bands are, however, not detected when the oxidation takes place in CH_2Cl_2 . The aforementioned data are summarized in Table 5 and confirm analysis of the $E_{1/2}$ vs 4σ plots, i.e. that the site of oxidation of each (P)Co(NO) porphyrin (i.e., compounds 1–6 in CDCl_3 and 1–7 in CH_2Cl_2) involves the conjugated π ring system.^{36–38} The

(31) The use of silver salts for the generation of π -cation radicals of porphyrins, chlorins, and their nitrosyl derivatives has some precedent.^{32–34}

- (32) Saheli, A.; Oertling, W. A.; Babcock, G. T.; Chang, C. K. *J. Am. Chem. Soc.* **1986**, *108*, 5630.
- (33) (a) Ozawa, S.; Sakamoto, E.; Ichikawa, T.; Watanabe, Y.; Morishima, I. *Inorg. Chem.* **1995**, *34*, 6362. (b) Ozawa, S.; Sakamoto, E.; Watanabe, Y.; Morishima, I. *J. Chem. Soc., Chem. Commun.* **1994**, 935. (c) Ozawa, S.; Fujii, H.; Morishima, I. *J. Am. Chem. Soc.* **1992**, *114*, 1548.
- (34) Shimomura, E. T.; Phillippi, M. A.; Goff, H. M.; Scholz, W. F.; Reed, C. A. *J. Am. Chem. Soc.* **1981**, *103*, 6778.
- (35) Hu, S.; Spiro, T. G. *J. Am. Chem. Soc.* **1993**, *115*, 12029.
- (36) Further support for this view comes from our observation that the singly oxidized product of (T(*p*-CH₃)PP)Co(NO) in CH_2Cl_2 containing TBAH shows a broad band centered at 776 nm, a value that is in the range characteristic of TPP π -cation radicals.³⁷
- (37) Fuhrhop, J.-H. *Struct. Bonding (Berlin)* **1974**, *18*, 1–67.
- (38) The ESR spectrum of singly oxidized (T(*p*-CH₃)PP)Co(NO) is characterized by an isotropic signal at $g = 2.009$ with a peak-to-peak separation of 18 G, a feature characteristic of cobalt tetraphenylporphyrin cation radicals.³⁹
- (39) (a) Ohya-Nishiguchi, H.; Khono, M.; Yamamoto, K. *Bull. Chem. Soc. Jpn.* **1981**, *54*, 1923. (b) Ichimori, K.; Ohya-Nishiguchi, H.; Hirota, M.; Yamamoto, K. *Bull. Chem. Soc. Jpn.* **1985**, *58*, 623.

Table 5. NO Vibrational Frequencies (cm^{-1}) of $[(\text{P})\text{Co}(\text{NO})]^n$ ($n = 0$ or $+1$) in CH_2Cl_2 , 0.2 M TBAH

compd no.	substituent	σ	$E_{1/2}$ (1st oxidn), V vs SCE	ν_{NO}			
				neutral	singly oxidized		
					EC ^a	AgBF ₄ ^b	NOBF ₄ ^b
1	<i>p</i> -OCH ₃	-0.27	0.89	1679	1724	1723	1724 (1293) ^c
2	<i>p</i> -CH ₃	-0.17	0.91	1679	1722	1724	1725 (1291) ^c
3	<i>m</i> -CH ₃	-0.07	0.93	1679	1718	1725	1726 (1294) ^c
4	H	0.00	0.96	1680	1726	1725	1726 (1293) ^c
5	<i>m</i> -OCH ₃	0.12	0.97	1682	1722	1725	1727 (1289) ^c
6	<i>p</i> -OCF ₃	0.35	1.06	1687	1730		1730 (...) ^d
7	<i>p</i> -CF ₃	0.55	1.14	1690	1730		1733 (...) ^e
8	<i>p</i> -CN	0.63	1.15	1693			

^a Singly oxidized product generated by electrochemical means. ^b Singly oxidized product generated by chemical means. ^c These bands in parentheses are also observed when the (P)Co compounds are reacted with NOBF₄ in CDCl₃. ^d The marker bands at *ca.* 1290 cm^{-1} are obscured by porphyrin bands. ^e The cation of compound 7 is produced in CH_2Cl_2 but not in CDCl₃.

previously reported electrochemistry of (TPP)Co(NO) in CH_2Cl_2 containing TBAP also supports this view.⁴⁰

Morishima has reported that imidazole coordination to nitrosyl Fe(II) chlorin and bacteriochlorin π -cation radicals produces Fe^{II}(NO⁺) complexes via valence isomerization.^{33c} Furthermore, Chang and Babcock have oxidized (OEP)Co^{II} to the π -cation radical [(OEP[•])Co^{II}]ClO₄, which is converted to [(OEP)Co^{III}-(ROH)₂]ClO₄ by addition of water or methanol.³² On the basis of our IR studies, we have not as yet been able to detect any valence isomerizations between the porphyrin-oxidized [(P[•])Co(NO)]⁺ and NO-oxidized [(P)Co(NO⁺)]. However, this effect cannot be excluded for our compounds, and further investigations in this direction are now in progress.

IR Spectroelectrochemistry in CH_2Cl_2 . The NO stretching vibrations of each neutral and singly oxidized compound are summarized in Table 5. The neutral complexes show a ν_{NO} which falls in the range 1679–1693 cm^{-1} , while the singly oxidized derivatives show a ν_{NO} band between 1718 and 1733 cm^{-1} , independent of the method used for generation of the oxidized products or nature of the counteranion (PF₆⁻ in the case of electrochemical generation and BF₄⁻ in the case of chemical generation). A value of ν_{NO} for [(T(*p*-CN)PP)Co(NO)]⁺ could not be determined since, as mentioned above, this product adsorbs at the electrode surface. Attempts to characterize the doubly oxidized products of the (P)Co(NO) porphyrins were also unsuccessful due to instability of the dications which undergo a rapid loss of NO on the time scale of the spectroelectrochemical experiments.

Time-dependent FTIR spectra were obtained during the first electrooxidation of compounds 1–7, and a representative example of the data is shown in Figure 5 for (T(*m*-OCH₃)PP)Co(NO) in CH_2Cl_2 containing 0.2 M TBAH. As seen in this figure, the 1682 cm^{-1} NO band of the initial complex decreases in intensity upon oxidation as a new band grows in at 1722 cm^{-1} . The ν_{NO} band of the singly oxidized product is 40 cm^{-1} higher than the ν_{NO} band of the neutral compound. A similar difference between the ν_{NO} of the neutral compound and the ν_{NO} of the singly oxidized product has been reported for cobalt and iron nitrosyl porphyrins or porphyrin-like compounds which are oxidized at the macrocycle,^{5b,12a,41} and the spectral changes in Figure 5 suggest that (T(*m*-OCH₃)PP)Co(NO) undergoes a one-electron abstraction from the π ring system. (T(*m*-OCH₃)PP)Co(NO), like (T(*p*-OCH₃)PP)Co(NO), contains a bent Co–N–O unit, and the small shift of the NO frequency

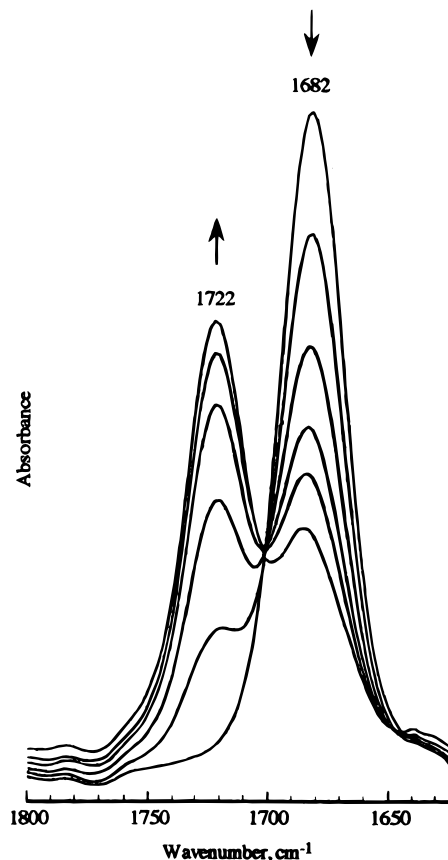


Figure 5. Time-dependent FTIR spectra measured between 1800 and 1620 cm^{-1} during oxidation of (T(*m*-OCH₃)PP)Co(NO) at a controlled potential of 1.2 V in CH_2Cl_2 , 0.2 M TBAH.

upon going from (T(*m*-OCH₃)PP)Co(NO) to its singly oxidized product suggests that the π -cation radical, [(T(*m*-OCH₃)PP[•])Co(NO)]⁺, should also exhibit a bent rather than linear Co–N–O unit. This result can be extended to the π -cation radicals of compounds 1–4, 6, and 7, for which the ν_{NO} is only 39–46 cm^{-1} higher than the ν_{NO} of their respective neutral precursors.

The first oxidation of (T(*m*-OCH₃)PP)Co(NO) is reversible on the cyclic voltammetry time scale, and this is also the case on the thin-layer spectroelectrochemical time scale, as shown by the disappearance of the 1722 cm^{-1} band of the singly oxidized product and a concomitant increase of the 1682 cm^{-1} band of the neutral compound as the potential is switched back to 0.0 V and maintained at this value for a few minutes. (T(*m*-OCH₃)PP)Co(NO) can thus be regenerated upon re-reduction of [(T(*m*-OCH₃)PP)Co(NO)]⁺ by both electrochemical and chemical means (using Cp₂Co as a reducing agent). This result

- (40) (a) Kadish, K. M.; Mu, X. H.; Lin, X. Q. *Inorg. Chem.* **1988**, 27, 1489. (b) Mu, X. H.; Kadish, K. M. *Inorg. Chem.* **1990**, 29, 1031. (c) Kelly, S.; Lancon, D.; Kadish, K. M. *Inorg. Chem.* **1984**, 23, 1451. (41) Autret, M.; Will, S.; Van Caemelbecke, E.; Lex, J.; Gisselbrecht, J.-P.; Gross, M.; Vogel, E.; Kadish, K. M. *J. Am. Chem. Soc.* **1994**, 116, 9141.

is also observed for all of the other compounds but $(\text{T}(p\text{-CN})\text{PP})\text{Co}(\text{NO})$.

Acknowledgment. G.B.R.-A. acknowledges the National Institutes of Health Institutional Development Award Program (Grant 1-P20-RR09180-01) for funding. The support of the Robert A. Welch Foundation (K.M.K., Grant E-680) is also gratefully acknowledged. S.J.H. acknowledges the Patricia Roberts Harris Fellowship Program for a graduate stipend, and

the authors thank Dr. V. Adamian for carrying out preliminary electrochemical experiments on these compounds.

Supporting Information Available: A listing of experimental crystallographic details for $(\text{T}(p\text{-OCH}_3)\text{PP})\text{Co}(\text{NO})$, a drawing showing the disorder of the nitrosyl group, and tables of anisotropic displacement parameters, hydrogen coordinates and isotropic displacement parameters, and deviations from the porphyrin carbon and nitrogen planes (9 pages). Ordering information is given on any current masthead page.

IC960031O